

Bottom-Up Design and Synthesis of Limit Size Lipid Nanoparticle Systems with Aqueous and Triglyceride Cores Using Millisecond Microfluidic Mixing

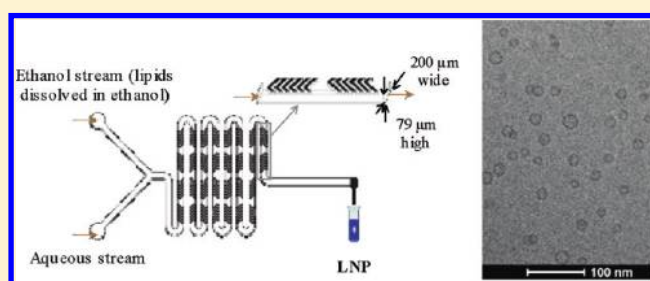
Igor V. Zhigaltsev,^{*,†} Nathan Belliveau,^{†,‡} Ismail Hafez,[†] Alex K. K. Leung,[†] Jens Huft,[§] Carl Hansen,[§] and Pieter R. Cullis[†]

[†]Department of Biochemistry and Molecular Biology, Faculty of Medicine, University of British Columbia, BC, Canada

[‡]Precision NanoSystems, Vancouver, BC, Canada

[§]Department of Physics and Astronomy, University of British Columbia, BC, Canada

ABSTRACT: Limit size systems are defined as the smallest achievable aggregates compatible with the packing of the molecular constituents in a defined and energetically stable structure. Here we report the use of rapid microfluidic mixing for the controlled synthesis of two types of limit size lipid nanoparticle (LNP) systems, having either polar or nonpolar cores. Specifically, limit size LNP consisting of 1-palmitoyl, 2-oleoyl phosphatidylcholine (POPC), cholesterol and the triglyceride triolein were synthesized by mixing a stream of ethanol containing dissolved lipid with an aqueous stream, employing a staggered herringbone micromixer. Millisecond mixing of aqueous and ethanol streams at high flow rate ratios (FRR) was used to rapidly increase the polarity of the medium, driving bottom-up synthesis of limit size LNP systems by spontaneous assembly. For POPC/triolein systems the limit size structures consisted of a hydrophobic core of triolein surrounded by a monolayer of POPC where the diameter could be rationally engineered over the range 20–80 nm by varying the POPC/triolein ratio. In the case of POPC and POPC/cholesterol (55/45; mol/mol) the limit size systems achieved were bilayer vesicles of approximately 20 and 40 nm diameter, respectively. We further show that doxorubicin, a representative weak base drug, can be efficiently loaded and retained in limit size POPC LNP, establishing potential utility as drug delivery systems. To our knowledge this is the first report of stable triglyceride emulsions in the 20–50 nm size range, and the first time vesicular systems in the 20–50 nm size range have been generated by a scalable manufacturing method. These results establish microfluidic mixing as a powerful and general approach to access novel LNP systems, with both polar or nonpolar core structures, in the sub-100 nm size range.



1. INTRODUCTION

Size matters in drug delivery. For long-circulating drug delivery systems, particle diameter is the most important determinant of biodistribution following intravenous (i.v.) injection. Long-circulating lipid nanoparticles (LNP) of diameter 100 nm or smaller are able to preferentially accumulate at disease sites such as tumors, and at sites of infection and inflammation, due to their ability to extravasate through the leaky vasculature in such regions.¹ Polymer-based nanoparticles (PNP) smaller than approximately 50 nm diameter can further permeate through the lymphatics² and accumulate in tissues such as bone marrow. PNP of 30 nm or smaller can access progressively more tissues in the body including poorly vascularized tumors.^{3,4} Below approximately 8 nm particles are quickly cleared by the kidney.⁵ Particles in the size range 10–50 nm are therefore the most potent in accessing extravascular target tissues and the synthesis of such systems is of intense interest for biomedical applications.

LNP systems used for drug delivery systems have primarily utilized vesicles of 80–100 nm diameter, largely because of the

availability of methods, such as extrusion of multilamellar vesicle (MLV) systems through polycarbonate filters,⁶ for making LNP in this size range. Methods for making limit size LNP, which can be substantially smaller than 80 nm, have not progressed significantly for over 30 years. The most commonly used method is sonication,⁷ which is a “top down” approach where micrometer-sized MLV are first formed by dispersion of lipid in water, followed by sonication to produce limit size systems. For lipid systems consisting of unsaturated phosphatidylcholine (PC), sonication of preformed MLV results in limit size vesicular LNP with diameters as small as 20 nm.^{8,9} However, sonication has many limitations including sample contamination, lipid degradation and, most importantly, lack of scalability. Other techniques to produce limit size LNP include “bottom up” approaches whereby LNP are formed by condensation of lipid from solution rather than by disrupting

Received: December 7, 2011

Revised: January 17, 2012

Published: January 23, 2012

larger structures. Examples include dilution of lipids dissolved in ethanol by rapid injection of the ethanol solution into a vigorously stirred aqueous buffer.¹⁰ This process can produce LNP as small as 25 nm diameter but is difficult to scale and suffers from poor reproducibility due to variable injection and mixing rates. With regard to nanoemulsions consisting of PC and fats such as triglycerides, the production of stable limit size systems with size ranges less than 50 nm diameter has proven elusive by any technique.¹¹

Here we show that rapid microfluidic mixing enables the “bottom-up” synthesis of well-defined limit size LNP systems with aqueous and triglyceride cores. By using a staggered herringbone microfluidic mixing device (SHM)^{12,13} (Figure 1)

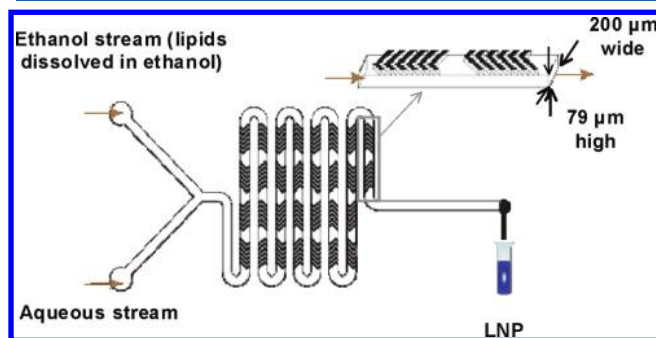


Figure 1. Schematic of LNP formulation process employing the SHM. Lipid in ethanol is pumped into one inlet and aqueous buffer into the other inlet of the microfluidic mixing device using a syringe pump. Herringbone structures induce chaotic advection of the laminar streams causing rapid mixing of the ethanol and aqueous phases and correspondingly rapid increase in the polarity experienced by the lipid solution. At a critical polarity lipid precipitates form as LNP. Dimensions of the mixing channel were $200\ \mu\text{m} \times 79\ \mu\text{m}$, and the herringbone structures were $31\ \mu\text{m}$ high and $50\ \mu\text{m}$ thick.

we drive LNP formation by millisecond mixing of lipids dissolved in ethanol with an aqueous stream. Rapid mixing suppresses mass transport effects that lead to larger and heterogeneous lipid aggregation, enabling the robust synthesis of monodisperse suspensions of LNP having the smallest possible stable structures compatible with the molecular composition. The SHM device was used to generate LNP from three test systems, namely 1-palmitoyl-2-oleoyl PC (POPC), POPC/cholesterol mixtures and mixtures of POPC with the triglyceride triolein. At flow rates of 2 mL/min and higher, the SHM device achieves sufficiently high mixing rates to produce limit size LNP systems for pure POPC and mixtures of POPC with cholesterol and triolein. The limit size LNP systems formed from PC/triolein are colloidal systems with diameters as small as 20 nm, consisting of triglyceride cores surrounded by a POPC monolayer. We show that this size can be precisely engineered by adjusting the POPC/triolein ratio. The limit size systems formed from POPC and POPC/cholesterol mixtures are bilayer vesicles, again with diameters as small as 20 nm. We show that these vesicular systems can be loaded with weak base drugs such as doxorubicin and have exciting potential as ultrasmall drug delivery agents.

2. MATERIALS AND METHODS

2.1. Materials. 1-palmitoyl-2-oleoyl-*sn*-glycero-3-phosphocholine (POPC) was obtained from Avanti Polar Lipids (Alabaster, AL). 1,2,3-tri(*cis*-9-octadecenoyl) glycerol (triolein), cholesterol, sodium chloride,

ammonium sulfate and doxorubicin hydrochloride were from Sigma-Aldrich Canada Ltd. (Oakville, Ontario, Canada).

2.2. Micromixer Design and Fabrication. The micromixer used in this study is a chaotic mixer for continuous flow systems with the layout based on patterns of asymmetric grooves on the floor of the channel that induce a repeated sequence of rotational and extensional local flows resulting in rapid mixing of the injected streams (staggered herringbone micromixer (SHM)).¹² The device was produced by soft lithography, the replica molding of microfabricated masters in elastomer. The device features a $200\ \mu\text{m}$ wide and $79\ \mu\text{m}$ high mixing channel with herringbone structures formed by $31\ \mu\text{m}$ high and $50\ \mu\text{m}$ thick features on the roof of the channel (Figure 1). Fluidic connections were made with $1/32''$ I.D., $3/32''$ O.D. tubing that was attached to 21G1 needles for connection with syringes. Syringes of 1, 3, and 5 mL were generally used for inlet streams. A dual syringe pump (KD200, KD Scientific) was used to control the flow rate through the device.

2.3. LNP Generation. Lipids (POPC or POPC/cholesterol (55/45 molar ratio) for preparations of bilayer systems, POPC/triolein at different ratios for preparations of nanoemulsions) were dissolved in ethanol at 10 mg/mL of total lipid. The LNP were prepared by injecting the ethanol-lipid solution into the first inlet and an aqueous buffer (saline, 154 mM NaCl) into the second inlet of the micromixer (Figure 1). The appropriate flow rate ratios (FRR, ratio of aqueous stream volumetric flow rate to ethanolic volumetric flow rate) were set by maintaining a constant flow rate in the ethanolic channel and varying the flow rates of the aqueous channel (typically 0.5–4.5 mL/min). Aqueous dispersions of LNP formed this way were collected from the outlet stream resulting from the mixing of two adjacent streams and dialyzed against 154 mM saline to remove the residual ethanol.

2.4. Generation of POPC LNP Exhibiting an Ammonium Sulfate Gradient. Limit size vesicular POPC LNP containing ammonium sulfate were formed as described above except that saline was replaced with 300 mM ammonium sulfate solution (FRR 3, 10 mg/mL POPC in ethanolic solution). After formation, the LNP were dialyzed against 300 mM ammonium sulfate to remove ethanol and then concentrated to 10 mg/mL lipid with the use of the Amicon Ultra-15 centrifugal filter units (Millipore). An ammonium sulfate gradient was generated by exchanging the extravesicular solution with 154 mM NaCl, pH 7.4 on Sephadex G-50 spin columns.

2.5. Loading of Doxorubicin into LNP and Doxorubicin Assay Protocols. Doxorubicin hydrochloride was dissolved in saline at 5 mg/mL and added to the ammonium sulfate-containing LNP to give drug-to-lipid molar ratios of 0.05, 0.1, 0.2, 0.4, and 0.6. The samples were then incubated at $60\ ^\circ\text{C}$ for 30 min to provide optimal loading conditions. Untrapped doxorubicin was removed by running the samples over Sephadex G-50 spin columns prior to detection of entrapped drug.

Doxorubicin was assayed by fluorescence intensity (excitation and emission wavelengths 480 and 590 nm, respectively) with a Perkin-Elmer LS50 fluorimeter (Perkin-Elmer, Norwalk, CT), the value for 100% release was obtained by addition of 10% Triton X-100 to a final concentration of 0.5%. Phospholipid concentrations were determined by an enzymatic colorimetric method employing a standard assay kit (Wako Chemicals, Richmond, VA). Loading efficiencies were determined by quantitating both drug and lipid levels before and after separation of external drug from LNP encapsulated drug by size exclusion chromatography using Sephadex G-50 spin columns and comparing the respective drug/lipid ratios.

2.6. Particle Size Measurement. LNP were diluted to appropriate concentrations with saline and the mean particle size was determined by dynamic light scattering (DLS) using a NICOMP model 370 submicrometer particle sizer (Particle Sizing Systems, Santa Barbara, CA). The sizer was operating in the vesicle and solid particle modes to determine the size of the liposomes (POPC and POPC/cholesterol systems) and lipid core nanospheres (POPC/triolein systems), respectively.

2.7. Nuclear Magnetic Resonance Spectroscopy. Proton decoupled ^{31}P NMR spectra were obtained using a Bruker AVII 400

spectrometer operating at 162 MHz. Free induction decays (FID) corresponding to $\sim 10\,000$ scans were obtained with a $15\ \mu\text{s}$, 55-degree pulse with a 1 s interpulse delay and a spectral width of 64 kHz. An exponential multiplication corresponding to 50 Hz of line broadening was applied to the FID prior to Fourier transformation. The sample temperature was regulated using a Bruker BVT 3200 temperature unit. Measurements were performed at $25\ ^\circ\text{C}$.

2.8. Cryo-Transmission Electron Microscopy (cryo-TEM).

Samples were prepared by applying $3\ \mu\text{L}$ of PBS containing LNP at 20–40 mg/mL total lipid to a standard electron microscopy grid with a perforated carbon film. Excess liquid was removed by blotting with a Vitrobot system (FEI, Hillsboro, Oregon) and then plunge-freezing the LNP suspension in liquid ethane to rapidly freeze the vesicles in a thin film of amorphous ice. Images were taken under cryogenic conditions at a magnification of 29K with an AMT HR CCD side mount camera. Samples were loaded with a Gatan 70 degree cryo-transfer holder in an FEI G20 Lab6 200 kV TEM under low dose conditions with an underfocus of 5–8 μm to enhance image contrast.

3. RESULTS AND DISCUSSION

3.1. Microfluidic Mixing Can Produce Limit Size LNP Systems for POPC, POPC/Cholesterol, and POPC/Triolein Dispersions at High Flow Rate Ratios.

The formation of LNP by condensation from an ethanol solution as it is rapidly mixed with an aqueous solution is driven by the rapid increase in the polarity of the medium. Two factors that can influence the rate of increase in polarity are the rate of mixing and the ratio of aqueous to ethanol volumes that are being mixed. The rate of mixing of the aqueous and ethanol streams in the herringbone micromixer employed here increases with total flow rate (Belliveau et al., unpublished). It would therefore be expected that increasingly monodisperse limit size LNP should be generated as the ratio of the aqueous flow rate to the ethanol flow rate (the flow rate ratio, FRR) is increased, due to both more rapid mixing and increased dilution effects. This behavior is similar to mixing processes used to produce nanoparticles by precipitation¹⁴ where, if the mixing time is much smaller than the aggregation time scale, the solution becomes supersaturated and nucleation events dominate particle creation to produce the smallest sizes possible. In addition, at higher flow rate ratios the final ethanol concentration is reduced, thus reducing the production of larger LNP due to particle fusion and lipid exchange (Ostwald ripening) after complete mixing is achieved.

The first objective of this work was to determine whether the microfluidic mixing process was capable of generating limit size vesicular systems for the unsaturated phospholipid POPC, which are known to be approximately 20 nm in diameter,⁸ and then to explore the systems generated for mixtures of POPC with cholesterol (which is known to increase the limit size⁹) and triolein. LNP were formed by mixing ethanol (containing dissolved lipids) and aqueous (154 mM saline) streams where the flow rate of the ethanol stream was held constant (0.5 mL/min) and the flow rate of the aqueous phase was increased over the range 0.5–4.5 mL/min, corresponding to FRR ranging from 1 to 9. The total flow rate was therefore varied over the range 1–5 mL/min. As we have demonstrated elsewhere for mixing of dyes a flow rate of 2 mL/min at a FRR of 3 corresponds to mixing times of approximately 3 ms (Belliveau et al., unpublished).

The three lipid systems investigated were POPC and POPC/cholesterol (55:45; mol/mol) and mixtures of POPC and triolein at a 60:40 mol ratio. Aqueous dispersions of POPC and POPC/cholesterol form bilayer systems, whereas mixtures of

POPC and triolein can potentially form emulsions with the POPC forming an outer monolayer surrounding a core of the hydrophobic triolein. For such a structure the limit size would be expected to be sensitive to the POPC/triolein ratio. Assuming a POPC area per molecule of $0.7\ \text{nm}^2$,¹⁵ a POPC monolayer thickness of 2 nm and a triolein molecular weight of 885.4 and density of 0.91 g/mL, it is straightforward to show that a POPC/triolein ratio of 60/40 (mol/mol) would be expected to result in limit size particles of ~ 20 nm diameter if the triolein core model is correct.

As illustrated in Figure 2A, for POPC systems, limit size LNP with a diameter of ~ 20 nm as assayed by light scattering

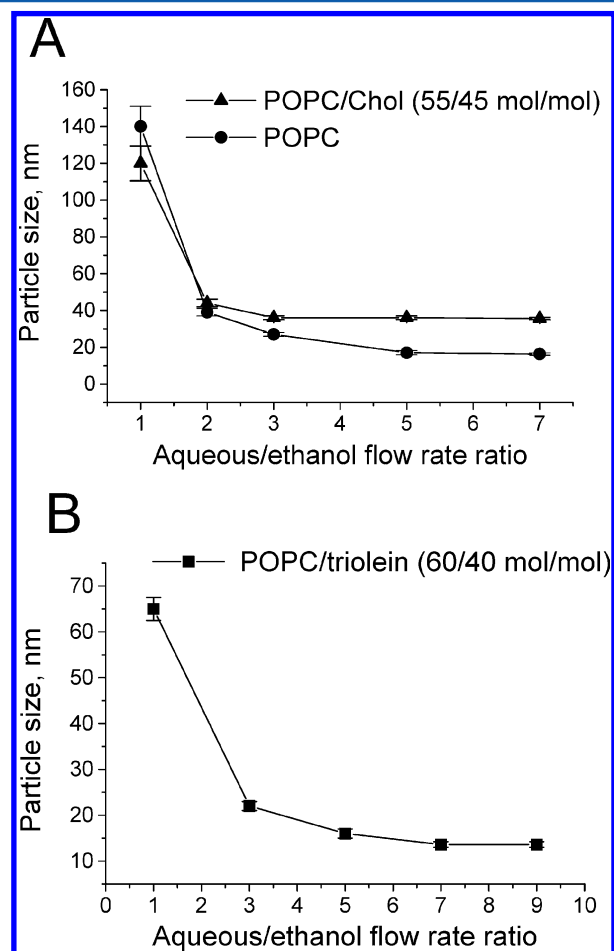


Figure 2. Microfluidic mixing can produce limit size LNP for POPC and mixtures of POPC with cholesterol or triolein. A. Limit size LNP can be formed from POPC and POPC/cholesterol (55/45; mol/mol) employing the staggered herringbone micromixer at higher flow rate ratios (FRR; aqueous-to-ethanol). B. Limit size systems can be formed from POPC and triolein at higher FRR. FRRs were varied by maintaining a constant flow rate in the ethanolic channel (0.5 mL/min) and increasing the flow rates of the aqueous channel from 0.5 to 4.5 mL/min. Size measurements were obtained using DLS (number weighting) as indicated under section 2.

(number mode) were observed for FRR of 3 and higher, in agreement with the limit sizes for LNP produced by sonication.⁸ The limit sizes detected by light scattering were dependent on the mode employed, for example the POPC limit size LNP diameter was 18 ± 7 (number-weighted), 28 ± 12 (volume-weighted), and 35 ± 14 nm (intensity-weighted); thus giving the polydispersity indices (PI) of 0.15–0.16 as

determined from the second order coefficient in the cumulants analysis provided by the light scattering instrument ($PI \approx (\sigma/\mu)^2$). The number-weighted value was used in this and subsequent experiments because the disproportionately large scattering intensity from a small number of larger LNP can skew light scattering size determinations and also because of the close correspondence between sizes obtained from the number mode determinations and those obtained from cryo-EM micrographs of LNP dispersions (see below). These dispersions were optically clear, consistent with the small size indicated by light scattering. For POPC/cholesterol mixtures limit size LNP with a diameter of ~ 40 nm (PI 0.17) were observed for FRR greater than 2 (Figure 2A). These results are in a good agreement with the previously observed⁹ size increase of limit size (sonicated) PC/cholesterol LNP compared to PC-based systems. Different sizes of limit size vesicular LNP obtained from different lipid compositions are to be expected as determined by the distribution of lipids across the membrane, the limiting radius of curvature of lipids composing the inner monolayer and the deformability of the bilayer as a whole.

In the case of POPC/triolein (60/40; mol/mol) mixtures, limit size LNP systems with a mean particle size slightly less than 20 nm diameter (PI 0.15) were observed for FRR greater than 3 (Figure 2B). Again, these small systems were optically clear. It should also be noted that LNP size was highly reproducible (within ± 2 nm) between different experiments and the LNP formed were highly stable. For example, no particle growth for the POPC/triolein nanoemulsions incubated at 20 °C in presence of 25% EtOH for at least 24 h was observed (data not shown). After dialysis to remove residual ethanol, the POPC/triolein 20 nm diameter systems remained stable for several months at room temperature.

3.2. ³¹P NMR and cryo-TEM Studies Indicate POPC and POPC/Cholesterol Limit Size LNP Form Bilayer Structures and POPC/Triolein Limit Size LNP Have Triglyceride Cores. ³¹P NMR techniques can be used to determine whether a fraction of the phospholipid is sequestered away from the bulk aqueous buffer, which would be consistent with bilayer vesicle structure, or whether all the POPC is in the outer monolayer, which would be consistent with a lipid core surrounded by a POPC monolayer. The ³¹P NMR signal arising from phospholipid in the outer monolayer can be quenched by adding Mn²⁺, which acts as a broadening agent to effectively eliminate the ³¹P NMR signal of phospholipid to which it has access.¹⁶ In the case of small unilamellar vesicles, this corresponds to the outer monolayer, where the ³¹P NMR signal is reduced by 50% or more upon addition of Mn²⁺. In the case of nanoemulsions of triglyceride stabilized by the presence of POPC, on the other hand, all the phospholipid would be expected to reside on the outer monolayer, and thus the entire ³¹P NMR signal should be quenched on exposure to Mn²⁺.

The ³¹P NMR spectra obtained for limit size LNP systems generated at a FRR of 3 for POPC, POPC/cholesterol, 55/45; mol/mol and POPC/triolein, 60/40; mol/mol in the absence and presence of 2 mM Mn²⁺ are shown in Figure 3A–C. In the absence of Mn²⁺, a sharp “isotropic” ³¹P NMR signal was observed in all three preparations (upper panels), consistent with the rapid isotropic motional averaging effects due to vesicle tumbling and lipid lateral diffusion effects expected for limit size bilayer systems.¹⁷ The addition of Mn²⁺ reduced the signal intensity by more than 50% of the initial signal for the POPC and POPC/cholesterol systems (Figure 3A,B; lower panels), indicating the presence of very small unilamellar

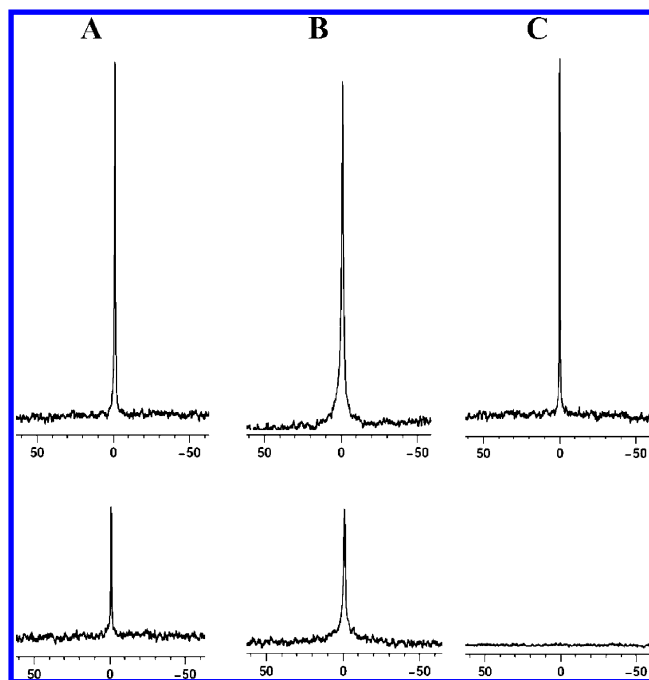


Figure 3. ³¹P NMR studies indicate limit size vesicular structures for POPC and POPC/cholesterol and limit size lipid core structure for POPC/triolein mixtures produced by microfluidic mixing. ³¹P NMR characterizations of POPC distributions in limit size LNP systems composed of (A) POPC; (B) POPC/cholesterol, 55/45; mol/mol and (C) POPC/triolein, 60/40; mol/mol. The upper panels show spectra in the absence of Mn²⁺ and the lower panels show spectra taken in the presence of 2 mM Mn²⁺. LNPs were produced at a FRR = 3 (3 mL/min for the aqueous stream, 1 mL/min for the ethanolic stream, total lipid concentration in the ethanol phase 10 mg/mL).

vesicles. The ratio of the lipid on the outside of the vesicle to the lipid on the inside (Ro/i) can be used to determine the vesicle size if the bilayer thickness and area per lipid molecule is known.⁹ The Ro/i for the POPC and POPC/cholesterol system can be calculated from Figure 3A,B to be 1.7 and 1.35, corresponding to sizes of approximately 30 and 50 nm diameter respectively for a bilayer thickness of 3.5 nm. These values are larger than determined by light scattering, which could arise due to increased packing density in the inner monolayer and/or the presence of a small proportion of multilamellar vesicles.

In the case of the POPC/triolein (60/40; mol/mol) limit size LNP systems, addition of Mn²⁺ resulted in the complete elimination of the ³¹P NMR signal (Figure 3C, lower panel). This is consistent with the presence of a nanoemulsion where all the POPC is located in outer monolayers surrounding hydrophobic triglyceride cores. There is no evidence of a population of bilayer vesicles as no residual signal from POPC on the vesicle interior was detected.

3.3. Cryo-TEM Can Be Used to Detect Both the Size and Internal Structure of LNP Systems. Cryo-TEM micrographs of bilayer vesicle systems reveal an electron dense lipid shell surrounding a less dense aqueous interior (see, for example,¹⁸), whereas systems with a hydrophobic core such as colloidal fat emulsions exhibit an electron dense interior.¹⁹ As shown in Figure 4A,B, limit size LNP composed of POPC and POPC/cholesterol (55:45; mol/mol) and formed by the microfluidic mixing technique (FRR = 3) exhibit the electron dense ring and less dense interior associated with unilamellar vesicle systems with an aqueous interior. In contrast, the limit

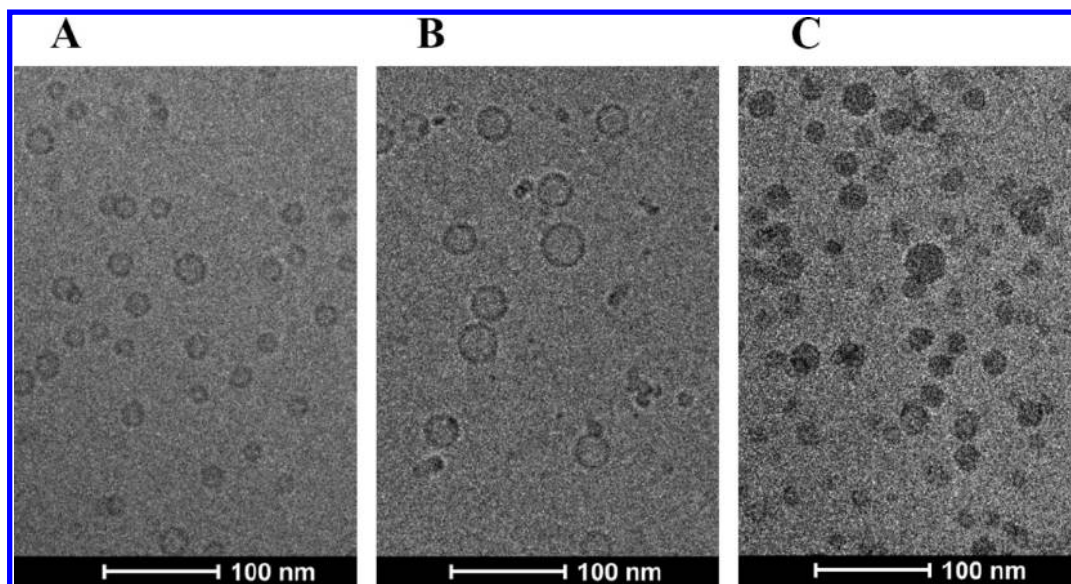


Figure 4. Cryo-TEM studies indicate limit size vesicular structures for POPC and POPC/cholesterol and limit size lipid core structure for POPC/triolein mixtures produced by microfluidic mixing. Cryo-TEM micrographs of limit size LNP composed of (A) POPC, (B) POPC/cholesterol; 55:45; mol/mol), (C) POPC/triolein, 60/40; mol/mol) produced at a FRR = 3 (3 mL/min for the aqueous stream, 1 mL/min for the ethanolic stream). The total lipid concentration in the ethanol phase was 10 mg/mL.

size LNP formed from POPC/triolein (60:40; mol/mol) exhibit an electron dense interior, consistent with the presence of a triglyceride core (Figure 4C).

The micrographs of Figure 4A–C also provide size information that can be used to validate the sizes determined by light scattering techniques. The sizes (means \pm SD) as determined by measuring the diameters of 200 LNP from cryo-TEM micrographs of limit size POPC, POPC/cholesterol (55:45;mol/mol) and POPC/triolein (60:40; mol/mol) were 19.5 ± 5 , 44.5 ± 13 , and 21.2 ± 9 nm, respectively, in good agreement with the sizes determined by light scattering (number-weighted).

3.4. Microfluidic Mixing Employing the Staggered Herringbone Mixer Offers a Powerful New Method for Production of Limit Size LNP with Nonpolar Cores. The synthesis of stable lipid core limit size 20 nm diameter LNP formed from POPC and triolein demonstrated here represents the first time such systems have been achieved. Microfluidic devices have previously been used to generate homogeneous emulsions by mixing two immiscible phases (oil and water),^{20–25} however these techniques result in micrometer-sized droplets; nanosized systems were not achieved. Sonication and other techniques^{11,26–31} have been used in attempts to generate lipid core nanoemulsions of 100 nm diameter or less with varying levels of success,^{11,31} diameters below 50 nm have not been achieved. Previous efforts (using sonication) to vary the size of PC/triolein dispersions by varying the proportions of these components have been frustrated by the production of mixtures of oil droplets and bilayer liposomes.¹¹ The only reported ability to produce lipid-containing nanoparticles of tunable size (35–180 nm) has been for lipid-polymer systems using hydrodynamic flow focusing.³² The success of the microfluidic mixing process can be attributed to the “bottom up” nature of the rapid mixing process. In particular, as the polarity of the water-miscible organic medium rises due to diffusional mixing with water, the most hydrophobic material may be expected to condense out of solution first, providing a hydrophobic nucleating structure that

is then coated by more polar lipids as they reach their solubility limits in the ethanol/water system. This suggests that the procedure will work best in situations where the material to be encapsulated is significantly less soluble in aqueous media than the coating lipid and where the encapsulated material is relatively insoluble in the coating lipid itself, as is the case for POPC/triolein mixtures.³³

As a demonstration of the power of microfluidic mixing for production of rationally engineered limit size LNP with a hydrophobic core, we examined the size of LNP formed from a variety of POPC/triolein ratios. This was driven by the remarkable correspondence between the 20 nm limit size observed for LNP produced from POPC/triolein 60:40; mol/mol mixtures and the theoretical size of 20 nm predicted on the basis of a structure where POPC forms a monolayer surrounding an internal triglyceride core. In addition to supporting the lipid core model, this observation suggests that it may be possible to engineer the size of POPC/triolein emulsions produced by microfluidic mixing by adjusting the molar ratios of phospholipid and triglyceride. The molar ratios of POPC/triolein required to form LNP of diameter 20, 40, 60, and 80 nm were calculated using the assumptions indicated above and used to produce limit size LNP employing the SHM at a FRR = 3. As shown in Table 1 there is excellent agreement between the predicted sizes over the range 20 nm–80 nm diameter and the measured sizes as determined by light scattering (number-weighted). It is probable that limit size LNP formulations of many hydrophobic molecules, including certain drugs, can be generated using this approach, where the size of the LNP is regulated by the hydrophobic core molecule to surface lipid ratio.

3.5. Microfluidic Mixing Offers a Powerful New Method for the Production of Limit Size Bilayer LNP with Significant Drug Delivery Potential. The use of the staggered herringbone micromixer to produce limit size vesicular LNP has major advantages compared to previous techniques. For example, an ultrasound-enhanced microfluidic mixing method³⁴ resulted in formation of vesicular systems

Table 1. Size of POPC/Triolein Systems Can Be Rationally Engineered by Adjusting the POPC-to-Triolein Ratio^a

lipid composition POPC/triolein (mol/mol)	predicted diameter (nm)	measured diameter (nm)
60/40	19	19.3 ± 2
52/40	30	26.7 ± 1.5
33/67	40	46.6 ± 0.6
22/78	60	61.3 ± 1.5
17/83	80	70 ± 3

^aThe predicted diameters for the various lipid compositions were calculated assuming that all the POPC was located in an outer monolayer surrounding an inner fat core composed of pure triolein. The calculation assumed a POPC area per molecule of 0.7 nm²,¹⁵ a POPC monolayer thickness of 2 nm and a triolein molecular weight of 885.4 and density of 0.91 g/mL. The measured diameters were determined by light scattering (number mode) using the Nicomp apparatus as described in section 2.

larger than 60 nm and approaches using hydrodynamic flow focusing^{35–37} generated vesicular LNP with diameters greater than 50 nm. In these latter protocols lipid was dissolved in isopropyl alcohol (IPPA) and the IPPA stream was hydrodynamically focused between two aqueous streams. The vesicle size decreased as the fluid rate ratio between the aqueous streams and the IPPA stream was increased, the smallest vesicles were obtained for a FRR of 60:1.³⁵ These results contrast with the results reported here using the staggered herringbone micromixer, which leads to the formation of limit size vesicular LNP with diameters as small as 20 nm at aqueous buffer-to-alcohol flow rate ratios as low as 3. The herringbone mixer provides an exponential increase in surface area between the two fluids with distance traveled, resulting in much faster diffusional mixing than the hydrodynamic flow focusing approach at equivalent flow rate ratios and correspondingly improved ability to generate limit size systems at lower FRR.

In comparison to previous techniques to produce limit size vesicular LNP, the microfluidic mixing technique is considerably less harsh than sonication and is more robust than the ethanol dilution method of Batzri and Korn,¹⁰ as mixing conditions can be precisely defined and controlled. In addition, as we have shown elsewhere (Belliveau et al., unpublished) the microfluidic mixing approach can be readily scaled simply by parallelization of mixing devices, achieving flow rates of 72 mL/min or higher.

With regard to potential drug delivery applications of limit size vesicular LNP systems, it is important to show that drugs can be loaded and retained in these extremely small systems. Doxorubicin, a widely used antineoplastic agent, was chosen as a model compound as it has been shown to be readily accumulated in bilayer liposomal systems in the 80–100 nm size range that exhibit a pH gradient, inside acidic.^{38–40} LNP systems composed of POPC were prepared at a FRR of 3 where the aqueous phase contained 300 mM ammonium sulfate, resulting in LNP with diameter 18 ± 7.0 nm as measured by light scattering (number mode). After removal of external ammonium sulfate, the LNP were incubated at 60 °C in presence of the varying amounts of doxorubicin corresponding to drug-to-lipid ratios of 0.05, 0.1, 0.2, 0.3, and 0.4 (mol/mol). As shown in Figure 5, loading efficiencies of approximately 100% were observed for drug-to-lipid ratios up to 0.2 (mol/mol), higher levels of available drug resulted in reduced loading efficiency. In all cases, drug loading was

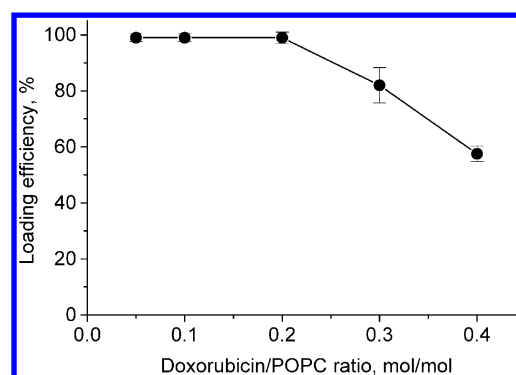


Figure 5. Doxorubicin can be efficiently loaded into limit size POPC LNP for drug-to-lipid ratios as high as 0.2 (mol/mol). Doxorubicin hydrochloride was dissolved in saline at 5 mg/mL and added to the ammonium sulfate-containing POPC LNP to give molar drug-to-lipid ratios of 0.05, 0.1, 0.2, 0.3, and 0.4 (mol/mol). The samples were then incubated at 60 °C for 30 min to provide optimal loading conditions. Untrapped doxorubicin was removed employing Sephadex G-50 spin columns prior to detection of entrapped drug as described in section 2.

achieved within 30 min with no increase in LNP size as compared to the empty precursors.

Extensive cryo-TEM studies on doxorubicin-loaded LNP in the 80–100 nm size range have demonstrated that accumulated doxorubicin precipitates into nanocrystals in the LNP interior, often resulting in a “coffee bean” appearance.⁴⁰ It was of interest to see whether internalized drug could be detected for the loaded limit size LNP; thus cryo-TEM studies on POPC LNP loaded with doxorubicin at drug-to-lipid ratios of 0.1 and 0.2 mol/mol were performed. Representative images are shown in Figure 6. Some indication of a coffee bean morphology can

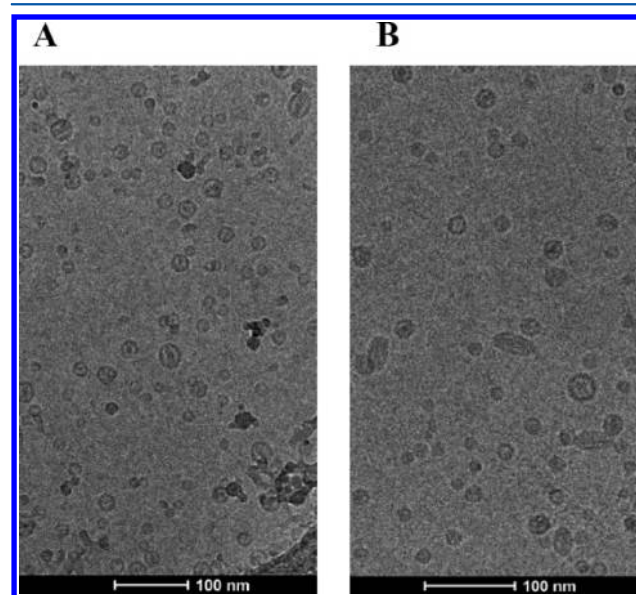


Figure 6. Limit size (20 nm diameter) LNP composed of POPC loaded with doxorubicin exhibit electron-dense cores. Cryo-TEM micrographs of POPC LNPs loaded with doxorubicin to achieve (A) doxorubicin/POPC drug-to-lipid molar ratios of 0.1 mol/mol and (B) doxorubicin/POPC drug-to-lipid molar ratios of 0.2 mol/mol. The bar represents 100 nm. For details of sample preparation and cryo-TEM protocols see section 2.

be observed for limit size LNP loaded at a 0.1 drug-to-lipid ratio (Figure 6A), however the bulk of the loaded LNP exhibit

an electron dense interior with no obvious structure. For LNP loaded at the higher drug-to-lipid ratio of 0.2 (mol/mol) the interior of the vesicles was uniformly electron dense, with no clearly defined structural organization (Figure 6B); although some particles appear distorted. However the bulk of the LNP are spherical with sizes that do not deviate significantly from empty limit size LNP. A size analysis based on a sample of ~150 LNP indicated sizes of 22 ± 8 and 22 ± 10 nm (mean \pm SD) for LNP loaded at drug-to-lipid ratios of 0.1 and 0.2 (mol/mol), respectively.

The high curvature of the lipid bilayer for limit size 20 nm diameter LNP systems raises concerns as to whether it provides a permeability barrier sufficient to stably retain encapsulated drug. The stability of the doxorubicin-loaded LNP stored at 4 °C was therefore monitored over 8 weeks. No detectable drug release or change in particle size was observed. For samples incubated at 37 °C, 90% (drug-to-lipid ratio 0.1 mol/mol) and 75% (drug-to-lipid ratio 0.2 mol/mol) of the loaded drug remained encapsulated at 24 h (data not shown).

The ability to load weak base drugs such as doxorubicin to high levels in limit size LNP is surprising given the extremely small interior volumes, which limits the amount of entrapped ammonium sulfate which provides the H⁺ ions required for protonation and consequent retention of weak base drugs after they diffuse into the vesicle interior. A straightforward calculation reveals that the maximum drug-to-lipid ratio that should be achievable for a 20 nm diameter vesicle containing 300 mM entrapped ammonium sulfate is 0.18 (mol/mol), assuming an area per POPC molecule of 0.7 nm² and a bilayer thickness of 4 nm.¹⁵ The reasonably complete encapsulation achieved for doxorubicin-to-lipid ratios of 0.2 (mol/mol) is therefore at the edge of what is theoretically possible, as indicated by reduced encapsulation efficiencies at higher drug-to-lipid ratios (Figure 5). The good retention properties of doxorubicin loaded limit size LNP can be attributed in part to precipitation of doxorubicin inside the LNP as reflected by the electron dense cores of the loaded LNP. As noted elsewhere, the presence of drug precipitates in LNP leads to dramatically improved retention properties.^{18,41} It is important to note that LNP loaded with drugs at drug-to-lipid ratios of 0.2 (mol/mol), which correspond to drug-to-lipid ratios of 0.15 (w/w) when expressed as weight doxorubicin/weight lipid, contain sufficient drug to be practical systems for therapeutic applications. For example, Doxil, the commercial formulation of doxorubicin, has a drug-to-lipid ratio of 0.125 (w/w).⁴²

The demonstrated ability to load and retain doxorubicin in limit size LNP systems in response to a pH gradient is a result that is likely to apply to all the members of the very large class of drugs that are weak bases containing primary, secondary or tertiary amines.³⁸ In addition, drugs such as docetaxel that are not weak bases can be loaded as pro-drug weak base derivatives.⁴³ As a result, it is probable that limit size LNP systems loaded with weak base drugs will form the foundation of a major new class of LNP therapeutics. This is because all previous clinically approved LNP drugs have diameters in excess of 50 nm, examples include Doxil (80 nm diameter⁴⁴) and Abraxane (130 nm⁴⁵). There are numerous reports indicating that while such large systems can often accumulate in regions of tumors there is little penetration into tumor tissue itself, which limits potency.^{46–51} This applies particularly to poorly vascularized tumors,⁴ where it has recently been shown that smaller (30 nm diameter) polymeric systems can

dramatically improve tumor penetration and potency as compared to systems with diameters 50 nm or larger. Extension of lipid nanoparticle technology, with advantages of biocompatibility, generalized methodology for optimizing drug loading and retention as well as extensive manufacturing and clinical experience, to LNP drugs with sizes as small as 20 nm may therefore be expected to have considerable clinical impact.

AUTHOR INFORMATION

Corresponding Author

*Telephone: (604) 822-4955. Fax: (604) 822-4843. E-mail: igorvj@mail.ubc.ca.

Notes

The authors declare no competing financial interest.

ACKNOWLEDGMENTS

This work was supported by the Canadian Institutes for Health Research (CIHR) through Grant FRN MOP 111213.

REFERENCES

- (1) Maeda, H.; Wu, J.; Sawa, T.; Matsumura, Y.; Hori, K. *J. Controlled Release* **2000**, *65*, 271–284.
- (2) Rao, D. A.; Robinson, J. R. *J. Controlled Release* **2008**, *132*, e45–e47.
- (3) Sarin, H. *J. Angiogenesis Res.* **2010**, *2*, 14–33.
- (4) Cabral, H.; Matsumoto, Y.; Mizuno, K.; Chen, Q.; Murakami, M.; Terada, Y.; Kano, M.; Miyazono, K.; Uesaka, M.; Nishiyama, N.; Kataoka, K. *Nat. Nanotechnol.* **2011**, *6*, 815–823.
- (5) Longmire, M.; Choyke, P. L.; Kobayashi, H. *Nanomedicine* **2008**, *3*, 703–717.
- (6) Hope, M. J.; Bally, M. B.; Webb, G.; Cullis, P. R. *Biochim. Biophys. Acta* **1985**, *812*, 55–65.
- (7) Huang, C. *Biochemistry* **1969**, *8*, 344–352.
- (8) De Kruijff, B.; Cullis, P. R.; Radda, G. K. *Biochim. Biophys. Acta* **1975**, *406*, 6–20.
- (9) De Kruijff, B.; Cullis, P. R.; Radda, G. K. *Biochim. Biophys. Acta* **1976**, *436*, 729–740.
- (10) Batzri, S.; Korn, E. D. *Biochim. Biophys. Acta* **1973**, *298*, 1015–1019.
- (11) Handa, T.; Saito, H.; Miyajima, K. *Biochemistry* **1990**, *29*, 2884–2890.
- (12) Stroock, A. D.; Dertinger, S. K. W.; Ajdari, A.; Mezic, I.; Stone, H. A.; Whitesides, G. M. *Science* **2002**, *295*, 647–651.
- (13) Squires, T. M.; Quake, S. R. *Rev. Mod. Phys.* **2005**, *77*, 977–1026.
- (14) D'Addio, S. M.; Prud'homme, R. K. *Adv. Drug Delivery Rev.* **2011**, *63*, 417–426.
- (15) Kucerka, N.; Tristram-Nagle, S.; Nagle, J. F. *J. Membr. Biol.* **2005**, *208*, 193–202.
- (16) Mayer, L. D.; Hope, M. J.; Cullis, P. R.; Janoff, A. S. *Biochim. Biophys. Acta* **1985**, *817*, 193–196.
- (17) Cullis, P. R. *FEBS Lett.* **1976**, *70*, 223–228.
- (18) Zhigaltsev, I. V.; Maurer, N.; Edwards, K.; Karlsson, G.; Cullis, P. R. *J. Controlled Release* **2006**, *110*, 378–386.
- (19) Kuntsche, J.; Horst, J. C.; Bunjes, H. *Int. J. Pharm.* **2011**, *417*, 120–137.
- (20) Zhang, B.; Tice, J. D.; Ismagilov, R. F. *Anal. Chem.* **2004**, *76*, 4977–4982.
- (21) Tan, Y. C.; Fisher, J. S.; Lee, A. I.; Cristini, V. A.; Lee, P. *Lab Chip* **2004**, *4*, 292–298.
- (22) Nisisako, T.; Torii, T.; Higuchi, T. *Lab Chip* **2002**, *2*, 24–26.
- (23) Anna, S. L.; Bontoux, N.; Stone, H. A. *Appl. Phys. Lett.* **2003**, *82*, 364–366.
- (24) Thorsen, T.; Roberts, R. W.; Arnold, F. H.; Quake, S. R. *Phys. Rev. Lett.* **2001**, *86*, 4163–4166.

- (25) Sugiura, S.; Nakajima, M.; Seki, M. *Langmuir* **2002**, *18*, 3854–3859.
- (26) Lundberg, B. *J. Pharm. Sci.* **1994**, *14*, 72–75.
- (27) Liu, F.; Liu, D. *Pharm. Res.* **1995**, *12*, 1060–1064.
- (28) Constantinides, P. P.; Chaubal, M. V.; Shorr, R. *Adv. Drug Delivery Rev.* **2008**, *60*, 757–767.
- (29) Sonnevile-Aubrun, O.; Simonnet, J.-T.; L'Alloret, F. *Adv. Colloid Interface Sci.* **2004**, *108–109*, 145–149.
- (30) Tadros, T.; Izquierdo, P.; Esquena, J.; Solans, C. *Adv. Colloid Interface Sci.* **2004**, *108–109*, 303–318.
- (31) Shah, P.; Bhalodia, D.; Shelat, P. *Syst. Rev. Pharm.* **2010**, *1*, 24–32.
- (32) Valencia, P. M.; Basto, P. A.; Zhang, L.; Rhee, M.; Langer, R.; Farokhzad, O. C.; Karnik, R. *ACS Nano* **2010**, *4*, 1671–1679.
- (33) Hamilton, J. A. *Biochemistry* **1989**, *28*, 2514–2520.
- (34) Huang, X.; Caddell, R.; Yu, B.; Xu, S.; Theobald, B.; Lee, L. J.; Lee, R. J. *Anticancer Res.* **2010**, *30*, 463–466.
- (35) Jahn, A.; Vreeland, W. N.; DeVoe, D. L.; Locascio, L. E.; Gaitan, M. *Langmuir* **2007**, *23*, 6289–6293.
- (36) Jahn, A.; Reiner, J. E.; Vreeland, W. N.; DeVoe, D. L.; Locascio, L. E.; Gaitan, M. *J. Nanopart. Res.* **2008**, *10*, 925–934.
- (37) Jahn, A.; Stavits, S. M.; Hong, J. S.; Vreeland, W. N.; DeVoe, D. L.; Gaitan, M. *ACS Nano* **2010**, *4*, 2077–2087.
- (38) Cullis, P. R.; Hope, M. J.; Bally, M. B.; Madden, T. D.; Mayer, L. D.; Fenske, D. B. *Biochim. Biophys. Acta Rev. Biomembr.* **1997**, *1331*, 187–211.
- (39) Mayer, L. D.; Bally, M. B.; Cullis, P. R. *Biochim. Biophys. Acta* **1986**, *857*, 123–126.
- (40) Li, X.; Hirsh, D. J.; Cabral-Lilly, D.; Zirkel, A.; Gruner, S. M.; Janoff, A. S.; Perkins, W. R. *Biochim. Biophys. Acta* **1998**, *1415*, 23–40.
- (41) Johnston, M. J. W.; Semple, S. C.; Klimuk, S. K.; Edwards, K.; Eisenhardt, M. L.; Leng, E. C.; Karlsson, G.; Yanko, D.; Cullis, P. R. *Biochim. Biophys. Acta* **2006**, *1758*, 55–64.
- (42) Drummond, D. C.; Meyer, O.; Hong, K.; Kirpotin, D. B.; Papahajopoulos, D. *Pharmacol. Rev.* **1999**, *51*, 691–743.
- (43) Zhigaltsev, I. V.; Winters, G.; Srinivasulu, M.; Crawford, J.; Wong, M.; Amankwa, L.; Waterhouse, D.; Masin, D.; Webb, M.; Harasym, N.; Heller, L.; Bally, M. B.; Ciufolini, M. A.; Cullis, P. R.; Maurer, N. *J. Controlled Release* **2010**, *144*, 332–340.
- (44) Gabizon, A. A. *J. Drug Target.* **2002**, *10*, 535–538.
- (45) Green, M. R.; Manikhas, G. M.; Orlov, S.; Afanasyev, B.; Makhson, A. M.; Bhar, P.; Hawkins, M. J. *Ann. Oncol.* **2006**, *17*, 1263–1268.
- (46) Uster, P. S.; Working, P. K.; Vaage, J. *Int. J. Pharm.* **1998**, *162*, 77–86.
- (47) Unezaki, S.; Maruyama, K.; Nagae, I.; Ishida, Y.; Nakata, M.; Ishida, O.; Iwatsuru, M.; Tsuchiya, S. *Int. J. Pharmacol.* **1996**, *144*, 11–17.
- (48) Kano, M.; Bae, Y.; Iwata, C.; Morishita, Y.; Yashiro, M.; Oka, M.; Fujii, T.; Komuro, A.; Kiyono, K.; Kaminishi, M.; Hirakawa, K.; Ouchi, Y.; Nishiyama, N.; Kataoka, K.; Miyazono, K. *Proc. Natl. Acad. Sci.* **2007**, *104*, 3460–3465.
- (49) Dreher, M. R.; Liu, W.; Michelich, C. R.; Dewhirst, M. W.; Yuan, F.; Chilkoti, A. *J. Natl. Cancer Inst.* **2006**, *98*, 335–44.
- (50) Perrault, S. D.; Walkey, C.; Jennings, T.; Fischer, H. C.; Chan, W. C. *Nano Lett.* **2009**, *9*, 1909–15.
- (51) Jain, R. K.; Stylianopoulos, T. *Nat. Rev. Clin. Oncol.* **2010**, *7*, 653–664.